

15 Abstract:

16 Ecologists often use time-series models to approximate dynamics arising from density
17 dependence, species interactions, community synchrony, and other processes. Dynamic
18 structural equation models can represent simultaneous and lagged interactions among variables
19 with missing data, and therefore encompasses a wide family of analyses (linear regression,
20 vector autoregressive models, and dynamic factor analysis). However, their interpretation as
21 structural causal models (i.e., counterfactual analysis) requires validating that the assumed
22 dynamics are consistent with available data. In site-replicated and phylogenetic contexts,
23 ecologists validate causal assumptions by testing implied conditional-independence relationships
24 (a directional-separation or “d-sep” test), but this has not been extended to include simultaneous
25 and lagged effects in time-series contexts. Here, we propose a time-series d-sep test and use a
26 simulation experiment and case studies to explore its performance. The simulation confirms that
27 this test results in a uniform p-value when using a correct causal model, and a low p-value (i.e., a
28 decision to reject a model) when the causal model is incorrect. As expected, time-series that are
29 short or have a large proportion of missing data then have less power to reject an incorrect
30 model. In a novel application involving pollock in the Gulf of Alaska, the test supports a
31 conceptual model where temperature drives spawning phenology, which subsequently affects
32 survey availability for a spawning survey. In a previously published analysis involving wolf-
33 moose interactions in Isla Royale, the test supports top-down control but cannot distinguish
34 whether bottom-up control is supported. We conclude that d-sep is a useful test to evaluate the
35 structural validity of a time-series model, allowing ecologists to make better causal inference
36 about dynamical systems from correlated time series data.

37

38 **Introduction**

39 Ecologists study causality in natural systems using controlled experiments and the analysis of
40 observational data (Grace, 2024; Siegel & Dee, 2025). Developing a well-formed hypothesis is a
41 key first step, and causal analysis have been proposed as a useful scientific framework to achieve
42 this (Grace & Irvine, 2020). Generating hypotheses is an iterative process of building graphical
43 causal networks (directed acyclical graphs; DAGs) of key variables in a system independent of
44 the data and prior to modeling, and this requires eliciting and representing expert knowledge
45 about ecological mechanisms (e.g., see Table 5 of Grace & Irvine, 2020). Structural causal
46 models (SCM) can then be used to estimate causal relationships by fitting statistical models to
47 DAGs (Pearl, 2009), and resolves well-known issues with bias when making causal statements
48 from predictive statistical models (Arif & MacNeil, 2022a) in particular when there are
49 unobserved confounding variables (Byrnes & Dee, 2025). SCMs are widely used outside of
50 ecology, and controlled experiments can be interpreted as a variant of SCM where some
51 variables (i.e., experimental treatments) are known to be independent of others. However,
52 ecologists also use observational data for systems that are not amenable to experimental
53 manipulation, and these settings require validating causal hypotheses to ensure unbiased causal
54 estimates (Arif & MacNeil, 2022b; Siegel & Dee, 2025). Thus, to advance understanding of
55 ecological mechanisms it is vital for analysts to be able to validate their causal models fitted to
56 observational time-series data.

57 Time-series dynamics pose particular challenges, because interactions among variables may
58 be either simultaneous (i.e., occurring much faster than the time-step in available observations)
59 or lagged. Lagged interactions result in temporal dependence, and dependence violates a key
60 statistical assumption of the popular structural equation model (SEM; Pearl, 2012) statistical

61 framework for estimating causal relationships. This then limits practical application of SEM to
62 time-series analysis. Thorson et al. (2024) extended the SEM modeling framework to allow for
63 correlated observations and lagged effects. This dynamic structural equation model (DSEM)
64 framework is efficiently represented as a Gaussian Markov random field and fitted as a
65 generalized linear mixed model, as implemented in the ‘dsem’ package (Thorson et al., 2024) in
66 the R statistical environment (R Core Team, 2023). DSEM encompasses a wide range of
67 statistical analyses including linear models, errors-in-variables, ARIMA models, dynamic factor
68 analysis, vector autoregressive models, and structural causal models. The DSEM framework
69 allows analysts to test novel causal hypotheses due to its decreased restrictions on data necessary
70 in a standard SEM, but it remains unclear how to validate them when fitted to (correlated)
71 observational data.

72 In general, the best way to validate a SCM is by using controlled experiments to confirm that
73 variables are independent conditional upon fixed conditions. However, experiments often cannot
74 be run at the scale of a system (due to logistical or legal constraints). Validating a SCM using
75 observational data generally involves testing whether the specified causal model is consistent
76 with available data. For example, consider a trophic cascade, where we might specify a SCM
77 where predator X affects consumer Y and consumer Y affects producer Z . We write this as two
78 causal paths: $X \rightarrow Y$ and $Y \rightarrow Z$. In this SCM, variation in predators is assumed to be
79 independent of producers, conditional upon a fixed value for consumers (i.e., $Z \perp X|Y$). We can
80 therefore test this conditional independence relationship as a regression ($Z = \beta_X X + \beta_Y Y + \epsilon$),
81 and if the slope β_X significantly departs from zero, then we can “reject” this component of SCM
82 as invalid. This insight is formalized by the directional-separation (“d-sep”) test (Shibley, 2000),
83 where all conditional-independence relationships implied by a given SCM are sequentially tested

84 and results are then combined in a single “omnibus” test. This d-sep test is widely used in the
85 analysis of controlled experiments (Meziane & Shipley, 2001) and phylogenetic comparative
86 analysis (von Hardenberg & Gonzalez-Voyer, 2013). The test has previously been extended to
87 multi-level models (Shipley, 2009), but has not to our knowledge been extended to time-series
88 analysis involving a combination of simultaneous and lagged interactions among variables.

89 We therefore address this by extending d-sep tests to measure whether a proposed time-series
90 structural model is consistent with available data. To address this, we first summarize the d-sep
91 test for path analysis, and then introduce modifications that are necessary for application to time-
92 series models that include simultaneous and lagged effects, or when dealing with missing data.
93 We then provide a simulation experiment to determine whether the proposed test performs
94 correctly (i.e., results in a uniform distribution for p-values) when the model is correctly
95 specified, and also how often it can reject an incorrectly specified model given different
96 simulation model structures, time-series lengths, and amounts of missing data. Finally, we use
97 two real-world case studies to illustrate the types of ecological inference that can be drawn from
98 the time-series d-sep test. Results suggest that the method performs well for simple (2-4
99 variable) models incorporating simultaneous and lagged effects given the range of time-series
100 that are common in population dynamics (25-100 time points), and the method is freely available
101 as function ``test_dsep(.)`` in the R package *dsem* for future use.

102 **Methods**

103 The Shipley (or d-sep) test can be applied to a directed acyclic graph (DAG) representing a
104 structural causal model. It proceeds by:

- 105 1. identifying the set of conditional independence (or “d-separation”) relationships that are
106 implied by the DAG. This set depends upon an *a priori* ordering of variables. Then for each

107 unique pair of variables, it identifies whether those variables are directly linked by the DAG.
 108 If that pair is not directly linked, the algorithm identifies the set of “conditioning variables”
 109 that (if held constant) would result in that pair then being independent. That pair of variables
 110 and the set of conditioning variables is then recorded as a “conditional independence
 111 relationship”. This step can be automated, and we use package *ggm* (Marchetti, 2006);
 112 2. fitting each d-separation relationship as a regression model, and extracting the p-value p_i
 113 associated with rejecting the null hypothesis for each conditional independence relationship
 114 from Step 1;
 115 3. combining these p-values using Fisher’s formula, $C = -2 \log(\sum_{i=1}^N p_i)$, and calculating an
 116 omnibus p-value under the assumption that C follows a chi-squared distribution with $2N$
 117 degrees of freedom.

118 We seek to generalize this method for application in time-series models that can include both
 119 simultaneous and lagged interactions among variables.

120 *Conditional independence in time-series modelling*

121 Next, we briefly summarize dynamic structural equation models (DSEM). For a set of $j \in$
 122 $\{1, 2, \dots, J\}$ variables over $t \in \{1, 2, \dots, T\}$ times, we define a matrix of latent variables \mathbf{X} with
 123 dimension $T \times J$. We can represent any set of simultaneous and lagged interactions by defining a
 124 path matrix $\mathbf{P}_{\text{joint}}$ with dimension $JT \times JT$, and defining a simultaneous equation:

$$125 \quad \text{vec}(\mathbf{X}) = \mathbf{P}_{\text{joint}} \text{vec}(\mathbf{X}) + \text{vec}(\mathbf{E})$$

$$126 \quad \text{vec}(\mathbf{E}) \sim \text{MVN}(\mathbf{0}, \mathbf{V}_{\text{joint}})$$

127 where \mathbf{E} is the $J \times T$ matrix of exogenous errors, and $\mathbf{V}_{\text{joint}}$ is the $JT \times JT$ covariance for these
 128 errors. Usefully, this simultaneous equation can be re-arranged as a Gaussian Markov random
 129 field:

130 $\text{vec}(\mathbf{X}) \sim \text{GMRF}(\mathbf{0}, \mathbf{Q})$

131 where $\mathbf{Q} = (\mathbf{I} - \mathbf{P}_{\text{joint}}^t) \mathbf{V}_{\text{joint}}^{-1} (\mathbf{I} - \mathbf{P}_{\text{joint}})$ is the sparse precision (inverse-covariance) matrix. The
 132 probability density of this GMRF can then be rapidly evaluated using the sparse precision \mathbf{Q} , and
 133 it can be fitted efficiently using the Laplace approximation as a Generalized Linear Mixed Model
 134 (GLMM).

135 The joint path matrix $\mathbf{P}_{\text{joint}}$ is formed by summing across simultaneous and lagged effects:

136
$$\mathbf{P}_{\text{joint}} = \underbrace{\mathbf{G}_0 \otimes \mathbf{P}_0}_{\text{Lag-0}} + \underbrace{\mathbf{G}_1 \otimes \mathbf{P}_1}_{\text{Lag-1}} + \dots$$

137 Where \mathbf{P}_0 is the $J \times J$ matrix of simultaneous (lag-0) interactions, \mathbf{P}_1 is the $J \times J$ matrix of lag-1
 138 interactions, \mathbf{G}_0 is a $T \times T$ matrix representing the lag-0 operator (i.e., an identity matrix), \mathbf{G}_1 is a
 139 $T \times T$ matrix representing the lag-1 operator (i.e., a matrix of 0s with a band of 1s one below the
 140 diagonal), \otimes is the Kronecker product, and we only show lag-0 and lag-1 interactions for
 141 simplicity of presentation. Similarly, we define the exogenous variance to only include
 142 simultaneous cross-correlations:

143
$$\mathbf{V}_{\text{joint}} = \mathbf{G}_0 \otimes (\mathbf{L}^t \mathbf{L})$$

144 Where \mathbf{L} can include variances (diagonal elements) and covariances (off-diagonal elements), and
 145 represents the Cholesky (i.e., square root) of simultaneous exogenous covariance $\mathbf{L}^t \mathbf{L}$. The
 146 model is completed by defining a distribution for data matrix \mathbf{Y} with dimensions $T \times J$. For each
 147 column \mathbf{y}_j , the user can specify that measurements are without error (i.e., $\mathbf{y}_j = \mathbf{x}_j$) or can specify
 148 a link function and distribution (i.e., $y_{tj} \sim f_j(g_j^{-1}(x_{tj}), \theta_j)$ where $g_j^{-1}(x_{tj})$ is the inverse-link
 149 function, θ_j is the estimated variance for measurement errors, and f_j is the distribution for
 150 errors). In the following, we focus upon the case of no measurement errors (i.e., $\mathbf{y}_j = \mathbf{x}_j$), which
 151 then collapses to a “process error” model.

152 This model then implies that the J variables \mathbf{x}_t in time t might depend upon \mathbf{x}_t but also \mathbf{x}_{t-1}
 153 in a model with a maximum lag of $M = 1$, where we use an “arrow-and-lag” notation e.g., $A \rightarrow$
 154 $B, 1$ to indicate that variable A in time t affects B in time $t + 1$. Therefore, the test for
 155 conditional dependence involves testing conditional independence relationships among a set of
 156 $J(M + 1)$ artificial variables, representing each variable j at each potential lag $m \in \{0, \dots, M\}$
 157 where M is the maximum lag included in the model. This insight yields a further complication.
 158 Say for a maximum lag of $M = 1$, variable $x_{t,j}$ and x_{t+1,j^*} might be independent only when
 159 conditioning upon preceding states x_{t-1,j^*} . To see this, consider a bivariate time-series model
 160 where A has a simultaneous (lag-0) impact on B , and both A and B exhibit first-order
 161 autocorrelation (e.g., Gompertz density dependence):

$$A \rightarrow B, 0$$

$$A \rightarrow A, 1$$

$$B \rightarrow B, 1$$

165 This implies that B is independent of the preceding A (i.e., path $A \rightarrow B, 1$ is zero) conditional
 166 upon lag-2 A (i.e., path $A \rightarrow B, 2$), lag-0 A (i.e., path $A \rightarrow B, 0$), and autoregressive effects of B
 167 (i.e., path $B \rightarrow B, 1$). This example therefore illustrates that for a maximum lag of M , we need to
 168 include conditioning variables for M times prior to the window of interest. In the case of $M = 0$
 169 (i.e., no lagged effects), then we can again ignore conditioning variables prior to the time-of
 170 interest, and the protocol collapses to the three steps in the standard d-sep test (see beginning of
 171 the Methods section).

172 To define conditional independence relationships in time-series models involving lags, we
 173 therefore define a “conditioning interval” with conditioning matrix \mathbf{A} . For the case of maximum
 174 lag $M = 1$, we have:

175

$$\mathbf{A} = \begin{bmatrix} \mathbf{P}_0 & 0 & 0 \\ \mathbf{P}_1 & \mathbf{P}_0 & 0 \\ 0 & \mathbf{P}_1 & \mathbf{P}_0 \end{bmatrix}$$

176 We then define all conditional-independent relationships within that conditioning matrix \mathbf{A} , in
177 this case using package *ggm*. However, we only keep those that define an independence
178 relationship between two variables that are both after the $M = 1$ “burn-in” intervals, while still
179 allowing conditioning variables to occur anywhere in the matrix. We then fit DSEM to each
180 conditional independence relationship independently, calculate the p-value for a two-sided Wald
181 test, and combine these using Fisher’s formula.

182 As further complication, we note that DSEM can account for missing data (i.e., $y_{tj} = \text{NA}$).
183 In these instances, we impute missing data from the predictive distribution of random effects
184 (i.e., their precision matrix \mathbf{H} given available data and fixed effects), and then use these imputed
185 data as “fixed” for each conditional-independence (CI) test. We explored alternative options
186 where we re-simulate missing data independently for each CI relationships, or used a single
187 imputed data set across all CI relationships for a given d-sep test. This exploration suggested
188 relatively little difference in performance, and we show the former in the following (see Table 1
189 for overview).

190 *Simulation experiment*

191 To explore the likely performance of this time-series d-sep test, we first conduct a factorial
192 simulation experiment. This involves 500 replicates of each combination of the following levels:
193 1. *Three simulation models*: We define three structural causal models. The simplest “sem” has
194 four variables and only simultaneous effects, where $A \rightarrow B$, $A \rightarrow C$, $B \rightarrow D$, and $C \rightarrow D$. The
195 intermediate involves two variables with simultaneous and lagged effects, where $A \rightarrow B$, and
196 an autoregressive process for both A and B . The most complicated involves four variables,

197 combining the same simultaneous effects as the “sem” scenario, but also including first-order
198 autocorrelation for each variable;

199 2. *Three sample sizes*: We simulate time-series of length $T = \{25,50,100\}$, representing short,
200 medium, and long ecological data sets;

201 3. *Five levels of missing data*: We randomly exclude data for each combination of variable and
202 year, with probability $p_{\text{missing}} = \{0,0.1,0.2,0.35,0.5\}$;

203 4. *Two estimation models*: For each combination of simulation model, sample size, and missing
204 data, we fit DSEM either using the true model structure, or using a mis-specified structural
205 model (see Fig. 1);

206 This design therefore involves $3 \times 3 \times 5 \times 2 \times 500 = 45,000$ applications of the time-series d-
207 sep test.

208 We assess two characteristics for the d-sep test in this experiment:

209 1. *Calibration*: A well-calibrated d-sep test will result in a uniform $U(0,1)$ distribution for p-
210 values when the simulation model matches the estimation model;

211 2. *Efficiency*: An efficient d-sep test will result in a large proportion of p-values that are close
212 to zero when the estimation model does not match the estimation model. Ideally, this p-value
213 will remain close to zero even when time-series are short, the simulation model is
214 complicated, and a large proportion of data are missing.

215 *Case study applications*

216 We also demonstrate the potential use of time-series d-sep via application to two real-world data
217 sets:

218 1. *Wolf-moose interactions on Isle Royale*: Building upon an analysis from Thorson et al.

219 (2024), we re-analyze a population census of wolves and moose on Isle Royale from 1959-

220 2019 (Vucetich & Peterson, 2012), where W and M are log-abundance. We fit a model with
221 just Gompertz density dependence ($W \rightarrow W, 1$ and $M \rightarrow M, 1$), adding bottom up interactions
222 ($M \rightarrow W, 1$), adding top-down interactions ($W \rightarrow M, 1$), or adding both;

223 2. *Spawning phenology and climate*: In a new example of DSEM, we use published data
224 representing spawning phenology for walleye pollock in the Gulf of Alaska from 1983-2023
225 and its relationship to survey availability (Rogers et al., 2025). This includes four variables,
226 representing sea surface temperature T , the average number of days between mean date of
227 spawning (as estimated from larval-derived hatch dates) and the mean date of a survey A , the
228 logit-transformed proportion of females $>30\text{cm}$ in a spawning or spent stage during the
229 spawning-grounds survey P , and the log-ratio Q between the surveyed biomass and predicted
230 biomass where the latter is taken from a population dynamics model fitted to the survey data
231 without accounting for timing or temperature (Monnahan et al., 2023). We explore three
232 alternative models for these data. The first (“temperature as driver”) views temperature as
233 the driver of all other variables (i.e., $T \rightarrow A$, $T \rightarrow P$, and $T \rightarrow Q$). The second (“regression
234 for availability”) views variables as independent predictors of survey availability (i.e., $T \rightarrow$
235 Q , $P \rightarrow Q$, and $A \rightarrow Q$). The third (“phenology as mediating effect”, described in Rogers et
236 al. 2025) claims that temperature affects survey availability via its mediating effect on
237 spawning phenology (i.e. $T \rightarrow A$, $A \rightarrow P$, and $A \rightarrow Q$). Across all three models, we also
238 estimate first-order autoregression for each variable (i.e., $T \rightarrow T, 1$, $A \rightarrow A, 1$, $P \rightarrow P, 1$, and
239 $Q \rightarrow Q, 1$) and assume that variables are measured without error (i.e., a process-error model)

240 In each case study, we record the p-value from the time-series d-sep test as well as the marginal
241 Akaike Information Criterion (AIC) for the fitted model.

242 **Results**

243 *Simulation experiment*

244 We first illustrate the performance (i.e., calibration and efficiency) of the d-sep test across
245 simulation models and time-series lengths when data are complete (Fig. 3). In the simulation
246 model without lagged effects (Fig. 3 top row), the correct model has an approximately uniform
247 $U(0,1)$ distribution for p-values across all sample sizes indicating that the d-sep test is well
248 calibrated. Similarly, the incorrect model results in a p-value < 0.1 in nearly all replicates,
249 indicating that the test is statistically efficient across sample sizes. Moving to the two-variable
250 model with lags (Fig. 3 middle row), we see that the correct model remains well calibrated across
251 sample sizes, but that the incorrect model only detects the mis-specification (i.e., a p-value $<$
252 0.1) in about 60% of the replicates at low sample sizes ($T = 25$), about 80% of replicates at
253 intermediate sizes ($T = 50$), before attaining good performance for long time-series ($T = 100$).
254 Finally, for the four-variable model with lags (Fig. 3 bottom row), we see that the test is poorly
255 calibrated (i.e., departs from a $U(0,1)$ distribution) for short time-series and incorrectly identifies
256 the model as mis-specified in nearly 40% of replicates. It then becomes well calibrated as the
257 time-series length increases. Expanding this experiment across different levels of missing data
258 (Fig. 4), we see that the simple estimation model remains well calibrated across the level of
259 missing data (Fig. 4 top row), but that the efficiency drops as p_{missing} increases from 0 to 50%.
260 A similar pattern holds for the other simulation models (Fig. 4 middle and bottom rows).
261 However, the decline in efficiency is notable at a lower value of p_{missing} in the intermediate-
262 complexity simulation model (Fig. 4 middle row), and the complex simulation model remains
263 poorly calibrated across levels of missing data for short sample sizes (Fig. 4 bottom-left panel,
264 red bullets).

265 *Case studies*

266 We also use two real-world case studies to illustrate the types of ecological inference that are
267 feasible when using d-sep to validate time-series models. In the case study involving predator-
268 prey interactions of moose and wolves in Isle Royale (Fig 5), we explored four models
269 corresponding to single-species (Gompertz) density-dependence, adding bottom-up or top-down
270 interactions individually, and adding both interactions jointly. The d-sep test then provides
271 strong evidence ($p < 0.01$) that the “bottom-up” model is incorrect, provides weak evidence
272 ($p = 0.15$) that the model with only density dependence is incorrect, and similar weight-of-
273 evidence for the remaining models. We therefore use AIC to conclude that the model with top-
274 down interactions is both validated and parsimonious relative to the model with both interactions
275 ($\Delta AIC = 1.1$). In the case study involving spawning phenology and survey availability for
276 pollock in the Gulf of Alaska (Fig. 6), we explored three models representing “temperature as
277 driver”, “regression for availability” or “phenology as mediating effect” hypotheses. The d-sep
278 test provides strong evidence ($p < 0.01$) against the validity of the first two models, but fails to
279 reject the third model ($p = 0.7$). We therefore conclude that this is the most appropriate
280 interpretation of those data given proposed hypotheses.

281 **Discussion**

282 Conditional independence (d-sep) testing is an established practice in structural equation models
283 and phylogenetic path analysis, and we provide a novel extension to time-series models that
284 include simultaneous and lagged interactions among variables. Our simulation experiment
285 confirms that the test is well calibrated, and that short time series ($T = 25$) can be sufficient for
286 simple structural models but that longer time series ($T = 100$) are required as model complexity
287 increases. Similarly, the model is statistically efficient, but this efficiency drops as the
288 proportion of missing data increases towards $p_{\text{missing}} = 0.5$. Finally, the case studies illustrate

289 that d-sep will in some cases retain several candidate models (i.e., for the Isle Royale data set),
290 such that model parsimony and multi-model averaging might be appropriate in these cases. In
291 other cases (e.g., involving pollock spawning phenology), the d-sep test provides quantitative
292 support for the ecological interpretation observational data.

293 Despite this progress in developing d-sep for time-series models, we have restricted
294 ourselves to scenarios involving 2-4 variables with simultaneous and first-order lags. We do this
295 because the limits of d-sep are already evident at this small model size. For example, using 4-
296 variables with lags and using short time series ($T = 25$), we already see poor calibration (i.e.,
297 rejecting the true model above intended rates). To understand this, consider that $J = 4$ variables
298 and one lag involves up to $\frac{2J(2J+1)}{2} = 36$ conditional independence relationships to test. The
299 number of CI relationships therefore grows as the square of the number of variables, and the d-
300 sep test seems to lose power rapidly for the sample sizes that are common when analyzing
301 annualized dynamics. Presumably this loss of statistical power is why previous simulation tests
302 of d-sep (e.g., in phylogenetic path analysis) have involved systems with < 5 variables (von
303 Hardenberg & Gonzalez-Voyer, 2013). To address this limit, we therefore envision that analysts
304 may choose to do some form of dimension reduction (e.g., dynamic factor analysis) on sets of
305 variables to identify a reduced set of composite variables, and testing the SCM validity for that
306 reduced set of variables. This procedure ultimately “masks” any concern about causal inter-
307 relationships among variables that are being combined in a single composite variable, and
308 therefore focuses statistical power on the remaining relationships of scientific interest.

309 We also note that d-sep is only test for significant linear relationships among variables, and
310 therefore cannot detect nonlinear or state-dependent relationships (unless they can be expressed
311 using lagged linear relationships). We therefore recommend further cross-comparison with

312 nonlinear causal analysis, e.g., using “empirical dynamic modelling” EDM (Munch et al., 2023).
313 EDM has proven to be powerful in detecting nonlinear causal systems, as validated via
314 microcosm experiments and methods comparisons (Chang et al., 2022; Sugihara et al., 2012).
315 However, EDM also appears to be more informative with longer time series. We therefore
316 envision a workflow using linear models (e.g., d-sep tests for a DSEM) when time-series are
317 relatively short, and comparison with a nonlinear method for longer time-series. We also
318 encourage further work estimating a linear “skeleton” within EDM models, so that EDM
319 collapses to linear interactions when data are limited, but can express a wide range of nonlinear
320 systems when data are abundant. Both DSEM and EDM involve fitting a Gaussian process
321 model, so it seems like their statistical integration would be feasible in future statistical research.

322 In summary, we recommend that d-separation be routinely tested for time-series models
323 when they are intended as structural causal models. When developing an SCM, we recommend
324 that only models with a priori ecological support that also pass the d-sep test be considered, and
325 that model parsimony or averaging then be considered for those models that are consistent with
326 data (i.e., pass the d-sep test). However, in models with 5+ variables and lagged dynamics, we
327 caution that d-sep appears to be poorly calibrated such that models may be erroneously rejected.
328 We therefore recommend ongoing research to refine methods for causal validation in ecological
329 systems, including methods to integrate experimental and observation studies. We hope that
330 these validation methods will help to unleash the potential for SCM in ecological systems.

331 **Data availability:**

332 Data for the pollock spawning phenology case study are from Rogers et al. (2025), available
333 online at https://github.com/larogers123/spawn_timing_catchability. Data for the Isle Royale are
334 from <https://www.isleroyalewolf.org/>, and we use the copy available in package *dsem*. Code to

335 reproduce case studies and the simulation experiment are available via GitHub
336 (https://github.com/James-Thorson-NOAA/dsep_in_dsem).

337 **Works cited:**

338 Arif, S., & MacNeil, M. A. (2022a). Predictive models aren't for causal inference. *Ecology*
339 *Letters*, 25(8), 1741–1745. <https://doi.org/10.1111/ele.14033>

340 Arif, S., & MacNeil, M. A. (2022b). Utilizing causal diagrams across quasi-experimental
341 approaches. *Ecosphere*, 13(4), e4009. <https://doi.org/10.1002/ecs2.4009>

342 Byrnes, J. E. K., & Dee, L. E. (2025). Causal Inference With Observational Data and
343 Unobserved Confounding Variables. *Ecology Letters*, 28(1), e70023.
344 <https://doi.org/10.1111/ele.70023>

345 Chang, C.-W., Munch, S. B., & Hsieh, C. (2022). Comments on identifying causal relationships
346 in nonlinear dynamical systems via empirical mode decomposition. *Nature*
347 *Communications*, 13(1), Article 1. <https://doi.org/10.1038/s41467-022-30359-8>

348 Grace, J. B. (2024). An integrative paradigm for building causal knowledge. *Ecological*
349 *Monographs*, 94(4), e1628. <https://doi.org/10.1002/ecm.1628>

350 Grace, J. B., & Irvine, K. M. (2020). Scientist's guide to developing explanatory statistical
351 models using causal analysis principles. *Ecology*, 101(4), e02962.
352 <https://doi.org/10.1002/ecy.2962>

353 Marchetti, G. M. (2006). Independencies induced from a graphical Markov model after
354 marginalization and conditioning: The R package ggm. *Journal of Statistical Software*,
355 15, 1–15.

356 Meziane, D., & Shipley, B. (2001). Direct and Indirect Relationships Between Specific Leaf
357 Area, Leaf Nitrogen and Leaf Gas Exchange. Effects of Irradiance and Nutrient Supply.
358 *Annals of Botany*, 88(5), 915–927. <https://doi.org/10.1006/anbo.2001.1536>

359 Monnahan, C. C., Adams, Grant D., Ferriss, B. E., Shotwell, S. Kalei, McKelvey, D.R., &
360 McGowan, David W. (2023). *Assessment of the walleye pollock stock in the Gulf of*
361 *Alaska* (Stock Assessment and Fishery Evaluation Report for Groundfish Resources of
362 the Gulf of Alaska). North Pacific Fishery Management Council. [https://apps-](https://apps-afsc.fisheries.noaa.gov/Plan_Team/2021/GOApollock.pdf)
363 [afsc.fisheries.noaa.gov/Plan_Team/2021/GOApollock.pdf](https://apps-afsc.fisheries.noaa.gov/Plan_Team/2021/GOApollock.pdf)

364 Munch, S. B., Rogers, T. L., & Sugihara, G. (2023). Recent developments in empirical dynamic
365 modelling. *Methods in Ecology and Evolution*, 14(3), 732–745.
366 <https://doi.org/10.1111/2041-210X.13983>

367 Pearl, J. (2009). Causal inference in statistics: An overview. *Statistics Surveys*, 3, 96–146.
368 <https://doi.org/10.1214/09-SS057>

369 Pearl, J. (2012). The causal foundations of structural equation modeling. In R. H. Hoyle,
370 *Handbook of structural equation modeling* (pp. 68–91). Guilford press.

371 R Core Team. (2023). *R: A Language and Environment for Statistical Computing*. R Foundation
372 for Statistical Computing. <https://www.R-project.org/>

373 Rogers, L. A., Monnahan, C. C., Williams, K., Jones, D. T., & Dorn, M. W. (2025). Climate-
374 driven changes in the timing of spawning and the availability of walleye pollock (*Gadus*
375 *chalcogrammus*) to assessment surveys in the Gulf of Alaska. *ICES Journal of Marine*
376 *Science*, 82(1), fsae005. <https://doi.org/10.1093/icesjms/fsae005>

377 Shipley, B. (2000). A New Inferential Test for Path Models Based on Directed Acyclic Graphs.
378 *Structural Equation Modeling: A Multidisciplinary Journal*, 7(2), 206–218.
379 https://doi.org/10.1207/S15328007SEM0702_4

380 Shipley, B. (2009). Confirmatory path analysis in a generalized multilevel context. *Ecology*,
381 90(2), 363–368. <https://doi.org/10.1890/08-1034.1>

382 Siegel, K., & Dee, L. E. (2025). Foundations and Future Directions for Causal Inference in
383 Ecological Research. *Ecology Letters*, 28(1), e70053. <https://doi.org/10.1111/ele.70053>

384 Sugihara, G., May, R., Ye, H., Hsieh, C., Deyle, E., Fogarty, M., & Munch, S. (2012). Detecting
385 Causality in Complex Ecosystems. *Science*, 338(6106), 496–500.
386 <https://doi.org/10.1126/science.1227079>

387 Thorson, J. T., Andrews III, A. G., Essington, T. E., & Large, S. I. (2024). Dynamic structural
388 equation models synthesize ecosystem dynamics constrained by ecological mechanisms.
389 *Methods in Ecology and Evolution*, 15(4), 744–755. [https://doi.org/10.1111/2041-](https://doi.org/10.1111/2041-210X.14289)
390 [210X.14289](https://doi.org/10.1111/2041-210X.14289)

391 von Hardenberg, A., & Gonzalez-Voyer, A. (2013). Disentangling evolutionary cause-effect
392 relationships with phylogenetic confirmatory path analysis. *Evolution; International*
393 *Journal of Organic Evolution*, 67(2), 378–387. [https://doi.org/10.1111/j.1558-](https://doi.org/10.1111/j.1558-5646.2012.01790.x)
394 [5646.2012.01790.x](https://doi.org/10.1111/j.1558-5646.2012.01790.x)

395 Vucetich, J. A., & Peterson, R. O. (2012). *The population biology of Isle Royale wolves and*
396 *moose: An overview*. www.isleroyalewolf.org

397

398

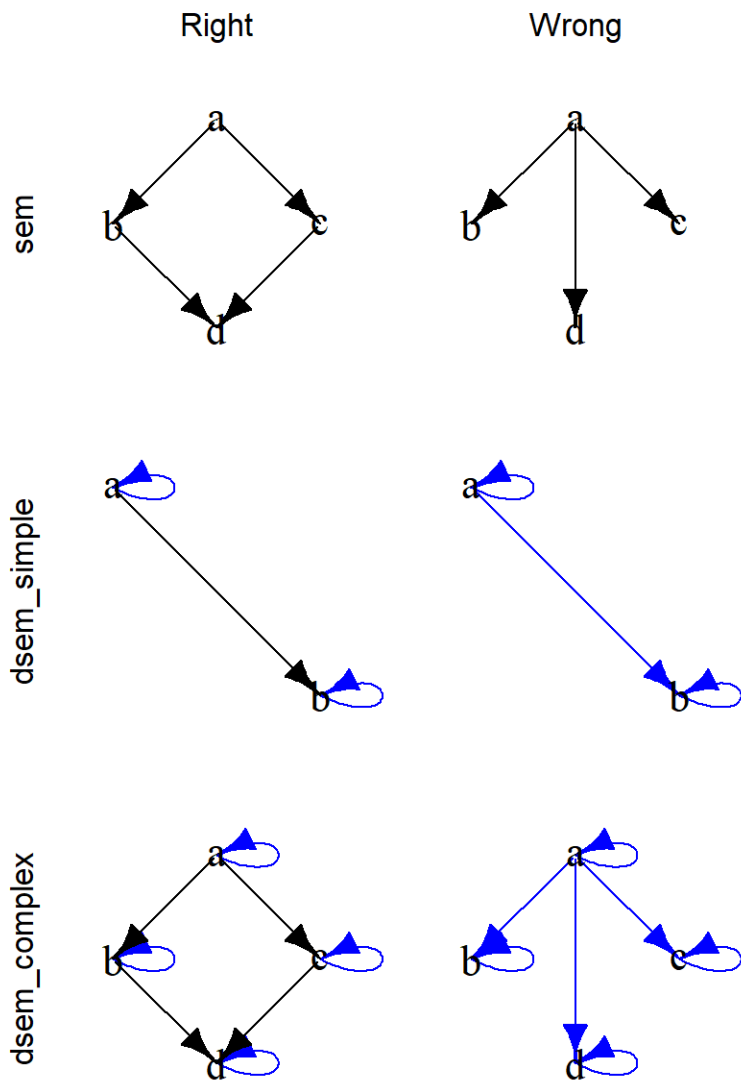
399 Table 1: Summarizing the steps required when extending the d-separation test for use in time-
400 series models that include both simultaneous and lagged relationships among variables.

Number	Title	Description
1	Extract path matrix	Extract path matrix, including initialization buffer for maximum number of lags
2	Define conditional independence relationships	Use “d-separation” to define the set of conditional independence (CI) relationships
3	Eliminate relationships	Filter CI relationships to eliminate duplicates, and restricting target and predictor variable to outside the initialization buffer (while allowing conditioning variables within the buffer)
4	Simulate missing data from predictive distribution	Simulate any missing data, either once across all CI tests or separately for each CI test
5	Fit CI relationships and combine p-values	Fit each CI relationship, recording the p-value for each individual CI test, and combining them using Fisher’s formula

401

402

403 Fig. 1: The structural causal model (SCM) used to simulate data (left column) in three
 404 simulation scenarios (rows), and the SCM that is specified when intentionally fitting with a
 405 mismatched SCM (right column). In each SCM, we show 2-4 time-series variables (labeled “a”
 406 through “d”), and causal paths showing either simultaneous effects (black arrows) or lag-1
 407 effects (blue arrows), where a blue arrow from a variable to itself (e.g., in the 2nd row) shows a
 408 first-order autoregressive effect.



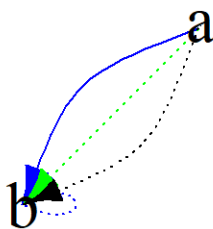
409

410

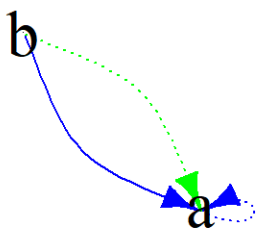
411 Fig 2: A visual depiction of the two conditional-independence (CI) relationships implied by the
412 “dsem_simple” structural causal model SCM (e.g., 2nd row left column of Fig. 1), as calculated
413 using conditioning matrix **A** (see Methods for structure). The CI relationship is shown with a
414 solid line, while the conditioning variables are shown as dashed lines. Given a time-series SCM
415 with maximum lag $M = 1$, the CI must condition upon a maximum of lag-2 relationships; e.g.,
416 the top CI relationship can be fitted as $b = \beta_0 \text{lag}(a, 1) + \beta_1 a + \beta_2 \text{lag}(a, 2) + \epsilon$ where we then
417 test for the significance of the β_0 coefficient.

Conditional independence 1

lag
■ 0
■ 1
■ 2



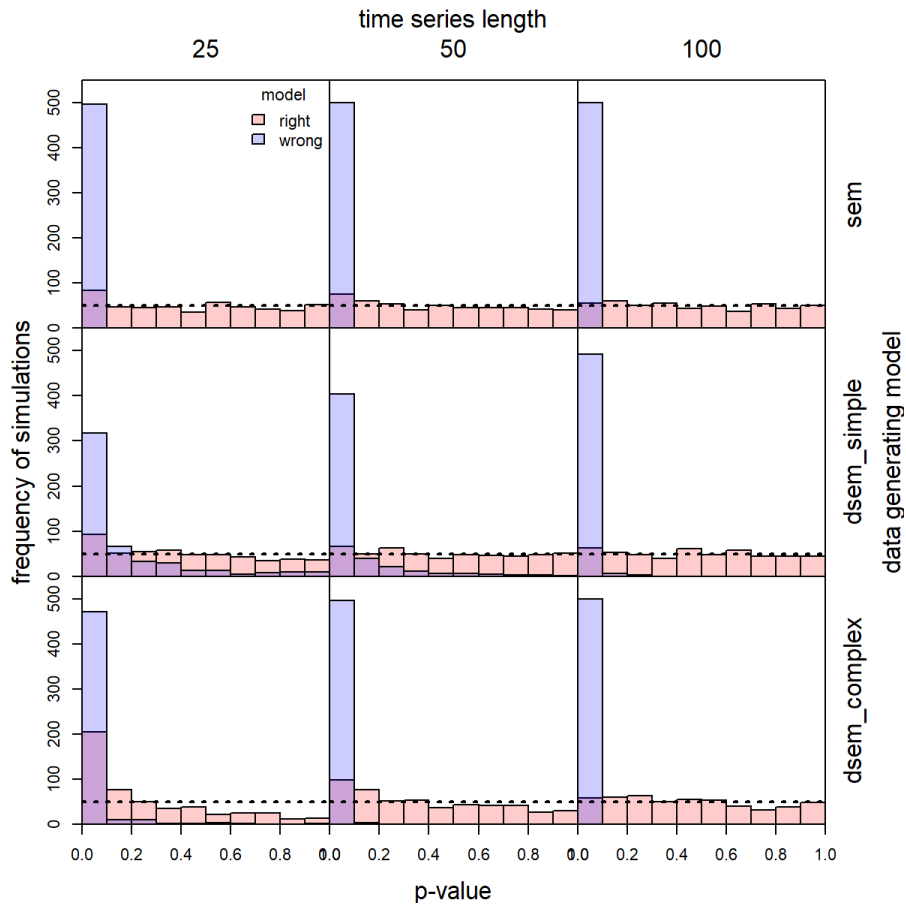
Conditional independence 2



418

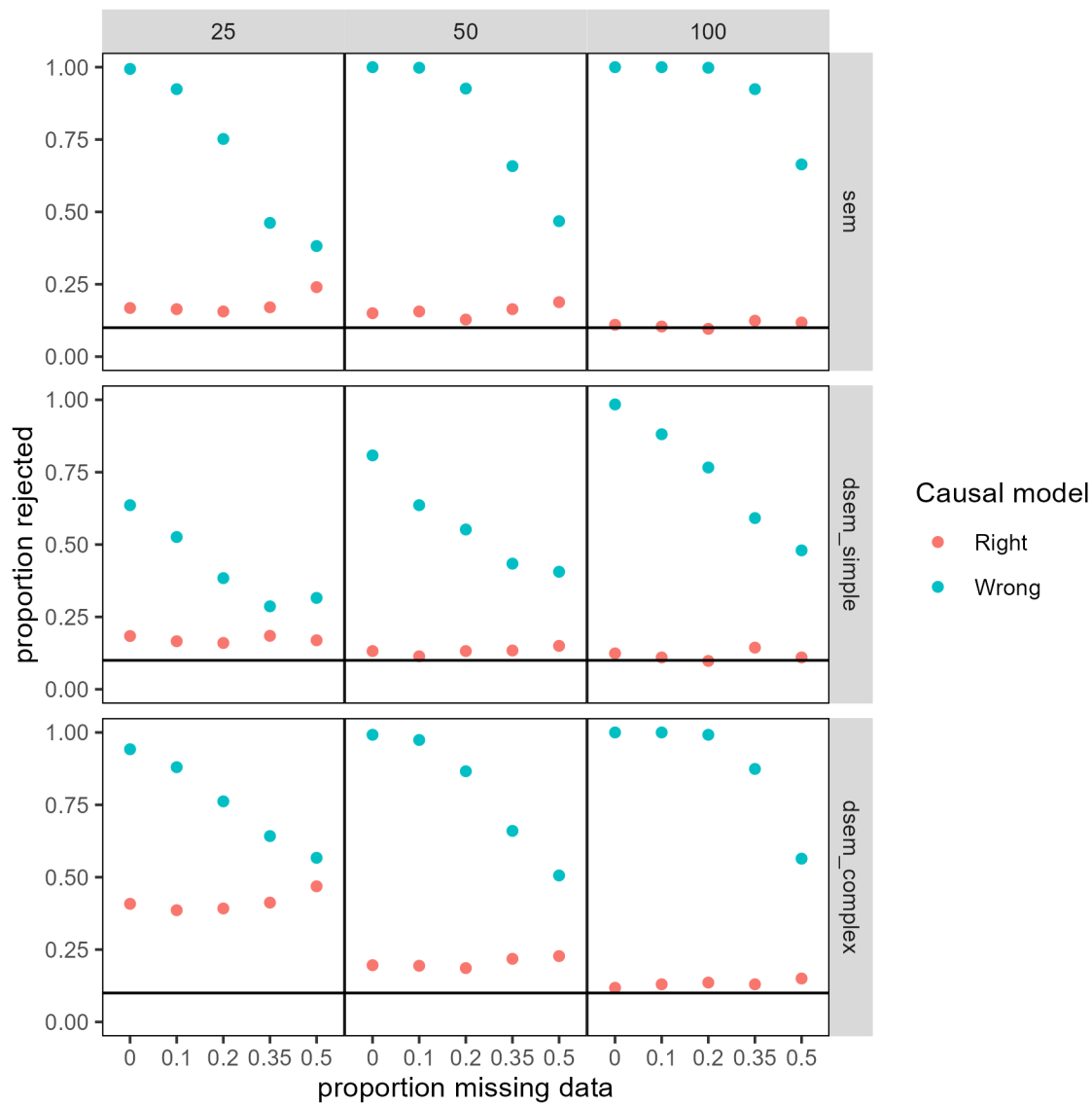
419

420 Fig. 3: Results from the simulation experiment showing the frequency of 500 replicates (y-axis)
 421 with a given p-value (x-axis) for a time-series d-separation test, while simulating time-series of
 422 length $T = \{25,50,100\}$ (columns) and using three structural causal models SCM (rows, see Fig.
 423 1 left column), and then refitting those simulated data with either the correct SCM (red
 424 histogram, Fig. 1 left column) or wrong SCM (blue histogram, Fig. 1 right column). A well-
 425 calibrated d-separation test will result in a p-value that follows a uniform $U(0,1)$ distribution
 426 (i.e., horizontal dashed line) when fitting the correct model, and an efficient test will result in a
 427 p-value that is close to zero when fitting a mis-specified model.

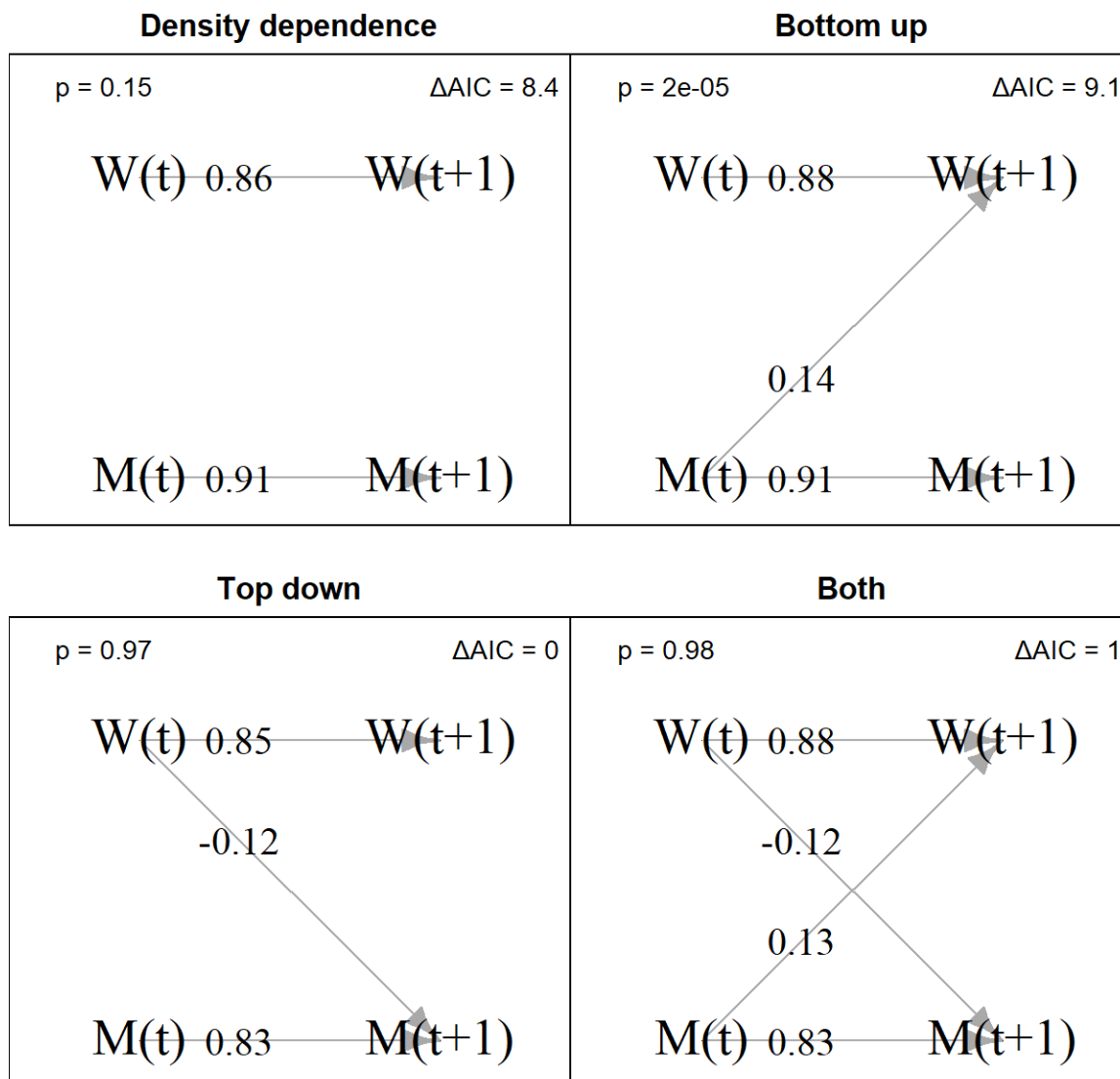


428

429 Fig. 4: Results from the simulation experiment when showing the proportion of simulation
 430 replicates with d-separation test resulting in $p < 0.1$ (y-axis) across five proportions of missing
 431 data $p_{\text{missing}} = \{0, 0.1, 0.2, 0.35, 0.5\}$ (x-axis), and across different time-series lengths (columns)
 432 and structural causal models SCMs (rows, see Fig. 3 caption for more details). A well-calibrated
 433 model with reject the test at nominal 0.1 rate (black horizontal lines) when the SCM is correct,
 434 and ideally will reject it at close to 1.0 rate when the SCM is incorrect.



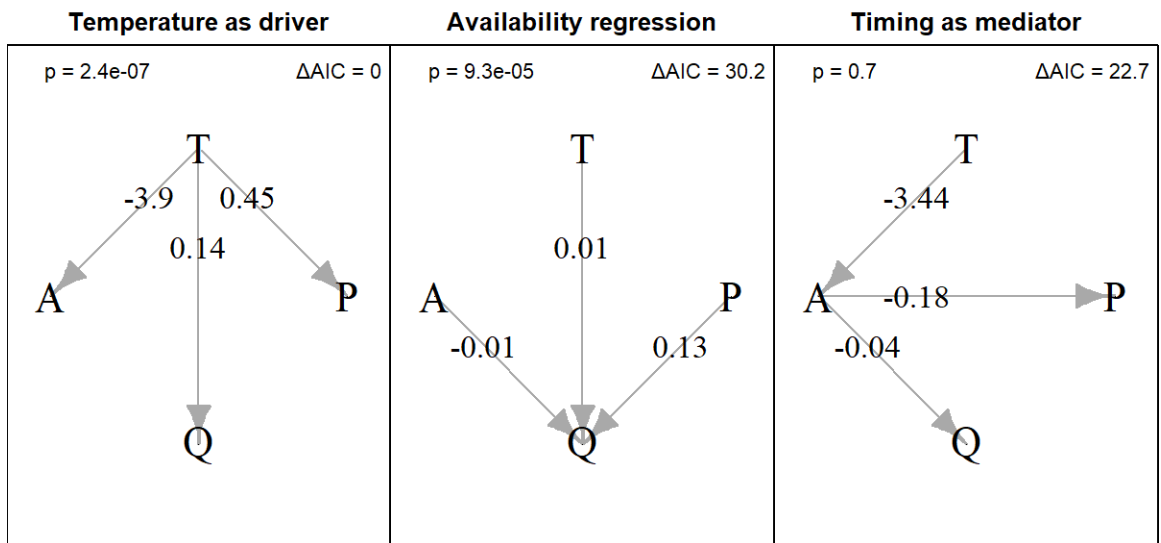
436 Fig. 5 – Estimated SCM showing a vector-autoregressive model fitting to data for wolf (W) and
 437 moose (M) log-abundance in Isle Royale 1959-2019 (Vucetich & Peterson, 2012). We compare
 438 a model with just Gompertz density dependence (i.e., $W \rightarrow W, 1$ and $M \rightarrow M, 1$), adding either
 439 bottom-up or top-down controls, or adding both jointly. For each model, we show the time-
 440 series d-sep test p-value (p, top-left corner) and the delta-marginal Akaike Information Criterion
 441 (top-right corner), where the most parsimonious model has $\Delta AIC = 0$.



442

443

444 Fig. 6: Estimated SCM showing the estimated path coefficient between temperature T , the
 445 average number of days between mean date of spawning and the mean date of a survey on
 446 spawning grounds A , the logit-transformed proportion of females $>30\text{cm}$ in a spawning or spent
 447 stage during the spawning-grounds survey P , and the log-ratio between the surveyed biomass
 448 and predicted biomass given other data Q . We show three SCMs (columns), either using
 449 temperature as an explanatory variable for all processes (“Temperature as driver”), using all
 450 variables to explain availability (“Availability regression”), or using survey timing as a
 451 mediating variable linking temperature to survey availability (“Timing as mediator”). We also
 452 show the time-series d-sep p-value (top left) and delta-marginal AIC (top-right) for each model.



453

454